

17. Hsu, Y. H., Shaw, C. K. & Chuong, C. M. Immunohistochemical localization of deleted-in-colon-cancer (DCC) protein in human epithelial, neural, and neuro-endocrine tissues in paraffin sections with antigen retrieval. *Kaohsiung J. Med. Sci.* **17**, 351–357 (2001).
18. Simon, T. C., Cho, A., Tso, P. & Gordon, J. I. Suppressor and activator functions mediated by a repeated heptad sequence in the liver fatty acid-binding protein gene (Fabpl). Effects on renal, small intestinal, and colonic epithelial cell gene expression in transgenic mice. *J. Biol. Chem.* **272**, 10652–10663 (1997).
19. Fearon, E. R. & Vogelstein, B. A genetic model for colorectal tumorigenesis. *Cell* **61**, 759–767 (1990).
20. Fodde, R. *et al.* A targeted chain-termination mutation in the mouse Apc gene results in multiple intestinal tumors. *Proc. Natl Acad. Sci. USA* **91**, 8969–8973 (1994).
21. Thiebault, K. *et al.* The netrin-1 receptors UNC5H are putative tumor suppressors controlling cell death commitment. *Proc. Natl Acad. Sci. USA* **100**, 4173–4178 (2003).
22. Tanikawa, C., Matsuda, K., Fukuda, S., Nakamura, Y. & Arakawa, H. p53RDL1 regulates p53-dependent apoptosis. *Nature Cell Biol.* **5**, 216–223 (2003).

Supplementary Information accompanies the paper on www.nature.com/nature.

Acknowledgements We wish to thank N. Gadot, C. Guix and G. Perret for excellent technical assistance. We also thank R. Fodde and S. Robine for advice and materials. This work was supported by the Ligue Contre le Cancer (P.M.), the Schlumberger Fondation (P.M.), the NIH (to P.M. and D.E.B.) and the Region Rhone-Alpes (to P.M. and J.Y.S.).

Competing interests statement The authors declare that they have no competing financial interests.

Correspondence and requests for materials should be addressed to P.M. (mehlen@univ-lyon1.fr)

A glycolipid of hypervirulent tuberculosis strains that inhibits the innate immune response

Michael B. Reed¹, Pilar Domenech¹, Claudia Manca², Hua Su^{1*}, Amy K. Barczak¹, Barry N. Kreiswirth³, Gilla Kaplan² & Clifton E. Barry III¹

¹Tuberculosis Research Section, NIAID, National Institutes of Health, 12441 Parklawn Drive, Rockville, Maryland 20852, USA

²Laboratory of Mycobacterial Immunity and Pathogenesis, ³Tuberculosis Center, Public Health Research Institute, 225 Warren Street, Newark, New Jersey 07103-3535, USA

* Present address: Laboratory of Human Bacterial Pathogenesis, NIAID, NIH, 903 South 4th Street, Hamilton, Montana 59840, USA

Fifty million new infections with *Mycobacterium tuberculosis* occur annually, claiming 2–3 million lives from tuberculosis worldwide¹. Despite the apparent lack of significant genetic heterogeneity between strains of *M. tuberculosis*^{2,3}, there is mounting evidence that considerable heterogeneity exists in molecules important in disease pathogenesis. These differences may manifest in the ability of some isolates to modify the host cellular immune response, thereby contributing to the observed diversity of clinical outcomes^{4–7}. Here we describe the identification and functional relevance of a highly biologically active lipid species—a polyketide synthase-derived phenolic glycolipid (PGL) produced by a subset of *M. tuberculosis* isolates belonging to the W-Beijing family⁸ that show ‘hyperlethality’ in murine disease models. Disruption of PGL synthesis results in loss of this hypervirulent phenotype without significantly affecting bacterial load during disease. Loss of PGL was found to correlate with an increase in the release of the pro-inflammatory cytokines tumour-necrosis factor- α and interleukins 6 and 12 *in vitro*. Furthermore, the overproduction of PGL by *M. tuberculosis* or the addition of purified PGL to monocyte-derived macrophages was found to inhibit the release of these pro-inflammatory mediators in a dose-dependent manner.

Phenotypically distinct isolates of *M. tuberculosis* are able to differentially manipulate the delicate balance that exists between

the pathogen and the human host^{4–6}. For example, a tuberculosis outbreak in a rural community of the United States caused considerable anxiety due to the large number of diagnostic skin test conversions in casual contacts of the index case. The *M. tuberculosis* strain isolated, CDC1551, was initially reported to be hypervirulent based on this fact. Subsequently, however, this strain was not found to be associated with higher than normal rates of active tuberculosis⁷. Consistent with the high rate of delayed-type hypersensitivity reaction in humans, infection of mice with CDC1551 results in an augmented immediate pro-inflammatory cytokine response, coupled with longer survival of infected animals^{4,5}. Strain HN878, in contrast, was isolated from an outbreak in the Texas prison system and has been responsible for at least three clusters of active disease². When this strain was used to infect mice, a hypervirulent phenotype resulted wherein mice failed to induce a strong TH₁-type T-cell and cytokine response early in infection and died much more rapidly^{5,6}. It has also been demonstrated that the robust cytokine-inducing activity of CDC1551 in the mouse lung is reproducible *in vitro* in human monocytes exposed to apolar lipid extracts from CDC1551 (ref. 5). This was the first experimental evidence to suggest that strain-related differences in host immune response and long-term disease outcome were directly attributable to unique lipid(s) produced by individual *M. tuberculosis* strains.

We postulated that the hypervirulent phenotype of strain HN878 might be associated with the lipid repertoire of this organism. In an attempt to identify lipids present in HN878 and absent from other

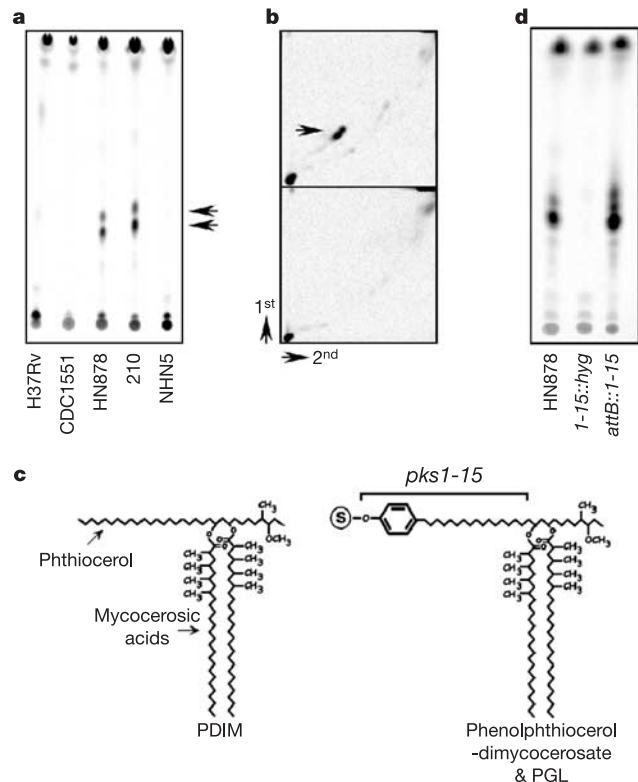


Figure 1 PGL is produced by HN878 and related W-Beijing strains. **a**, Lipids extracted from [¹⁴C]propionic-acid-labelled cultures of the strains indicated were analysed by TLC. The positions of the lipids specific to HN878 and 210 are highlighted (arrows). **b**, Lipids of [¹⁴C]propionic-acid-labelled HN878 (top panel) and *pks1-15::hyg* (bottom panel) were analysed by two-dimensional TLC, demonstrating loss of the HN878-specific lipids (arrow) in *pks1-15::hyg*. **c**, Model structures of PDIM and PGL. The region of PGL predicted to be derived from Pks1-15 (ref. 16) and the position of a variable number of carbohydrate residues (S) attached to the phenyl moiety are shown. **d**, TLC of lipids extracted from [¹⁴C]p-hydroxybenzoic-acid-labelled cultures including the complemented *attB::pks1-15* strain.

recent clinical isolates of *M. tuberculosis*, various strains were incubated in the presence of [1-¹⁴C]propionic acid to specifically radiolabel lipids possessing methyl branches. Two closely migrating species were identified by thin-layer chromatography (TLC) of apolar extracts of HN878 and W-Beijing strains 210, W10 and W4 (refs 8, 9), but not CDC1551, NHN5 (ref. 2) or the laboratory strain H37Rv¹⁰ (Fig. 1a and data not shown). This result was particularly intriguing because the 210 and W4 strains have also been shown to be associated with a diminished early pro-inflammatory cytokine response within infected human monocytes *in vitro* and hypervirulent behaviour in rodent models of infection¹¹ (G.K., unpublished data). Despite being isolated from distinct geographical regions of the United States, all of the W-Beijing strains examined (including HN878) have virtually indistinguishable IS6110 genotyping patterns¹¹.

The ability to label these lipids with propionate suggested that a polyketide synthase (PKS)-like enzyme capable of extension with methylmalonyl co-enzyme A was involved in their biosynthesis. Several polyketides have recently been described for *M. tuberculosis*, and in many cases represent methyl-branched lipids important for virulence^{12,13}. As part of an ongoing programme to identify

PKS-derived products in *M. tuberculosis*, a set of *pkc* hygromycin-replacement mutants was constructed in HN878, each of which was screened for the absence of the unique lipids identified above. In this way, we established that the HN878 strain disrupted within the

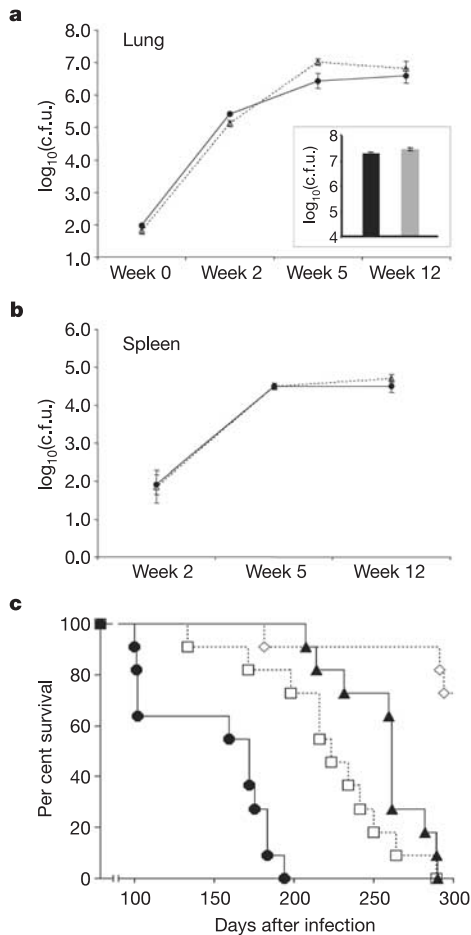


Figure 2 PGL is responsible for the hypervirulent phenotype of HN878 in mice. **a**, Six-week-old B6D2 F₁ mice were infected via aerosol with HN878 (solid line) and *pks1-15::hyg* (dotted line). At 3 h and 2, 5 and 12 weeks after infection lungs were homogenized and plated for c.f.u. determination (3–4 mice per group). Values are log₁₀(c.f.u.) (±s.e.m.). At necropsy, lung c.f.u. were obtained for HN878 (black column) and *pks1-15::hyg* (grey column) (inset). **b**, At 2, 5 and 12 weeks after infection spleens were homogenized and plated. **c**, Survival analysis was carried out for additional mice (11 mice per group) infected with HN878 (filled circles), H37Rv (open squares), *pks1-15::hyg* (filled triangles) and CDC1551 (open diamonds).

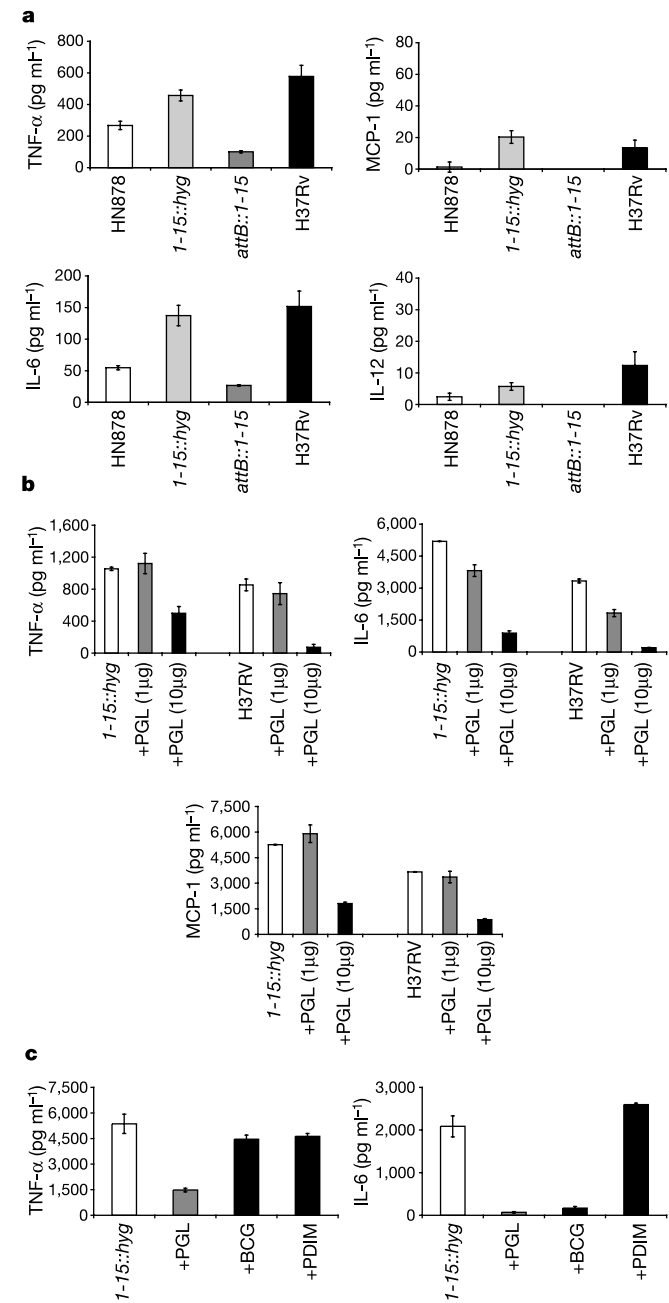


Figure 3 PGL-mediated inhibition of pro-inflammatory cytokine release by murine BMMs. **a**, Culture supernatants obtained 24 h after BMM infections were analysed by ELISA for the presence of the cytokines TNF-α, IL-6, IL-12 and the chemokine MCP-1. Data obtained from one representative experiment performed in triplicate are presented (±s.e.m.). **b**, BMMs were incubated for 24 h in the presence of increasing amounts of purified PGL (0, 1 or 10 μg) in addition to apolar lipids (5 μg) extracted from HN878 *pks1-15::hyg* and H37Rv. Culture supernatants were analysed by ELISA for TNF-α, IL-6 and MCP-1. IL-12 was unable to be detected in these lipid assays. PGL alone showed no effect in these assays. Representative data (±s.e.m.) from a single experiment performed in triplicate are presented. **c**, BMMs were incubated for 24 h in the presence of 2 μg purified PGL, *M. bovis* (BCG) PGL or PDIM in addition to apolar lipids (1 μg) extracted from HN878 *pks1-15::hyg*. Culture supernatants were analysed in triplicate (±s.e.m.) by ELISA for TNF-α and IL-6.

pksl-15 gene cluster (as annotated in the H37Rv genome¹⁰) no longer produced these lipid species (*pksl-15::hyg*; Fig. 1b). The identity of these lipids was suggested by the genomic context of *pksl-15* and became clear with the publication of the association between *pksl-15* and the production of a complex phenolic glycolipid¹⁴; however, no phenotype had been ascribed to mutants in this pathway.

In H37Rv and CDC1551, the absence of PGL production was confirmed to be associated with the previously reported 7-base-pair deletion resulting in a frameshift in what would otherwise be predicted to be a single gene encompassing *pksl* and *pksl5* (refs 14, 15). An intact *pksl-15* gene was identified for HN878, 210, W4 and W10 (data not shown) and, as predicted, each of these strains produces the unique lipids. Interestingly, the unrelated NHN5 strain fails to produce these lipids (Fig. 1a), yet doesn't contain the lesion resulting in their absence from H37Rv and CDC1551. This suggests that multiple independent genetic alterations may have led to the loss of production of such lipids, and may imply that their production is selected against within the existing population of *M. tuberculosis* strains.

pksl-15 is located in a region of the genome that includes the *mas*, *mmpL7* and *ppsA-E* genes, all of which are known to be involved in the formation or transport of phthiocerol dimycocerosate (PDIM). PDIM is a complex wax located in the outer wall of mycobacteria, loss of which has been associated with attenuation of *M. tuberculosis*^{12,16}. Importantly, PDIM synthesis and export were found to be unaffected in HN878 *pksl-15::hyg* (data not shown). A class of lipids structurally related to PDIM and collectively referred to as phenolic glycolipids (Fig. 1c) have been reported to be present in *Mycobacterium bovis*, *Mycobacterium leprae* and other pathogenic mycobacteria, including a limited number of *M. tuberculosis* isolates^{14,17}. Labelling of HN878 with [¹⁴C]*p*-hydroxybenzoic acid, a known precursor of PGL¹⁶, resulted in radioactive species co-migrating with the HN878-specific lipids labelled with [¹⁴C]propionate, confirming that the lipids contain a *p*-hydroxybenzyl constituent (Fig. 1d). ¹H-NMR spectroscopy (data not shown) was carried out on material purified by preparative TLC, confirming the presence of multiple sugars (chemical shift (δ) = 5.13 and 5.50 parts per million (p.p.m.)), phenolic protons (δ = 6.9–7.1 p.p.m.) and an esterified β -diol (δ = 4.84 p.p.m.), all consistent with the known structure of PGL¹⁸. Inactivation of *MmpL7*, a transmembrane protein shown to facilitate PDIM transport¹², blocked not only PDIM secretion as previously reported but also PGL secretion. Although the ratio of the individual PGLs is slightly altered, PGL synthesis is otherwise unaffected in this *MmpL7*-inactivation mutant, suggesting that attachment of sugar residues occurs before transport across the cell membrane (data not shown).

To address the role of PGL in tuberculosis infection and its association with the hypervirulent phenotype displayed by HN878 (ref. 6), we performed low-dose aerosol infections of BL6/DBA2 F₁ mice (50–100 colony-forming units (c.f.u.) per mouse) with HN878 and HN878 *pksl-15::hyg*. There was no significant difference in bacterial numbers within the lung over the initial 12 weeks of infection, yet there was an almost 90-day difference in median survival between the two groups ($P < 0.0001$) (Fig. 2). Indeed, the survival of mice infected with *pksl-15::hyg* was not significantly different to that of the intermediately virulent H37Rv^{5,6} ($P = 0.07$). No alteration in bacterial number in the spleen was observed, indicating that absence of PGL has no detrimental effect on bacterial dissemination in this model. Enumeration of bacteria at the time of necropsy confirmed that the difference in mouse survival is not attributable to differences in bacterial survival or bacillary load. A second set of infections carried out with a larger infecting inoculum (300–400 c.f.u. per mouse) confirmed the *pksl-15::hyg* phenotype. Despite the higher antigenic load in this case, a difference in median survival of 42 days ($P = 0.004$) was still observed (data not shown).

Diverse biological activities ranging from suppression of human

monocytic responses *in vitro* to a role in Schwann cell invasion have been attributed to the abundant PGL-1 of *M. leprae*^{19–24}. To explore the mechanism by which the production of PGL contributes to the hyperlethality observed in mice infected with HN878, we compared pro-inflammatory cytokine production in bone-marrow-derived macrophages (BMMs) infected with HN878, *pksl-15::hyg* and H37Rv. In addition, we included in these studies an HN878 *pksl-15::hyg* strain containing an intact copy of *pksl-15* under the control of the *hsp60* promoter on the integrative expression plasmid pMV361 (ref. 25). Examination of this strain, *attB::pksl-15*, confirmed that expression of *pksl-15* could fully restore PGL production and function to the HN878 *pksl-15::hyg* strain. On the basis of the incorporation of [¹⁴C]*p*-hydroxybenzoic acid, production of PGL within *attB::pksl-15* was three times greater than that of the parental HN878 strain (Fig. 1d). Infection of BMMs revealed an inverse correlation between PGL production and the level of secretion of the pro-inflammatory mediators tumour-necrosis factor- α (TNF- α , interleukin (IL)-6, IL-12 and MCP-1 (monocyte chemoattractant protein-1) (Fig. 3a). When comparing HN878 with the *pksl-15::hyg* mutant, the degree of inhibition due to the presence of PGL was typically in the order of 2–2.5-fold, depending on the particular cytokine assayed. Moreover, this PGL-mediated inhibition of the innate pro-inflammatory response is reflected in the poor survival of mice infected with wild-type HN878 (Fig. 2c). The cytokines IL-4, IL-10 and IL-13, often linked with TH₂-type allergic responses and an alternative pathway of macrophage activation²⁶, were not produced at detectable levels in these assays. Finally, we incubated BMMs with apolar lipids extracted from either *pksl-15::hyg* or H37Rv in the presence of increasing amounts of purified PGL. These experiments revealed a dose-dependent inhibition of pro-inflammatory cytokine release similar to that observed for BMMs infected with the PGL-producing strains HN878 and *attB::pksl-15* (Fig. 3b). The specificity of the response is highlighted by the fact that the structurally related PGL from *M. bovis* (BCG) bearing only a single carbohydrate substituent¹⁷ showed differential effects in terms of TNF- α and IL-6 secretion, whereas PDIM displayed no inhibitory activity (Fig. 3c).

PGL confers on a subset of *M. tuberculosis* isolates the ability to inhibit the release of key inflammatory effector molecules by cells of the host's innate immune response. Ultimately, this inhibition manifests itself in the hyperlethal phenotype observed in mice. So far, the link between PGL and hypervirulence is restricted to an experimental model that in many ways does not adequately reflect the pathology observed in human tuberculosis¹. Consequently, the role of PGL in human granulomatous tuberculosis disease remains to be determined. Of particular importance will be a careful examination of any linkage between PGL and the infection sequelae associated with the W-Beijing family, notably multidrug resistance, dissemination and outbreaks of disease^{8,9}. However, the results herein provide a clear demonstration that the spectrum of tuberculosis disease is likely to reflect not only variable host factors, but also the variable expression of bacterial factors including PGL. □

Methods

Bacterial strains and media

M. tuberculosis CDC1551 (T. Shinnik), H37Rv (American Type Culture Collection 27294), HN878 (J. Musser), NHN5 (J. Musser), W4 (TB Center collection) and 210 (D. Cave) were cultured using 7H9 liquid medium (Difco) containing 10% ADC (albumin dextrose complex), 0.5% glycerol and 0.1% Tween-80 or 7H11 agar containing 10% OADC (oleic acid plus ADC), 0.5% glycerol and 0.1% L-asparagine. Where necessary, media were supplemented with 50 $\mu\text{g ml}^{-1}$ hygromycin or 25 $\mu\text{g ml}^{-1}$ kanamycin.

Mutant construction

Using sense (5'-CAGATCTCGGCTGCTCAAT-3') and antisense (5'-GAGCCAGGACTGCAACACCT-3') primers specific for the H37Rv *pksl* sequence, a 1.9-kb fragment was amplified from H37Rv genomic DNA and cloned into pCR-Blunt (Invitrogen). The resultant plasmid was restricted with *Bst*EII and blunt-end ligated with the 1.3-kb hygromycin expression cassette from p16R1 (ref. 27). The *pksl::hyg* fragment was released from pCR-Blunt by digestion with *Eco*Rv and *Spe*I and inserted via blunt-end ligation into

BamHI-restricted pPR23-1 (ref. 28). Similarly, a 2.3-kb fragment was amplified using sense (5'-ATAAGAAATCGGCCCGCTGTGTCGAGCAATATCGACAG-3') and antisense (5'-GGACTAGTCCAGAGCCACTACCGTGAGCAAG-3') primers specific for the H37Rv *mmpL7* gene, digested with *NorI*, *SpeI* and cloned into pcDNA2.1 (Invitrogen). A 1.3-kb *NorI* fragment containing the hygromycin cassette of pHint²⁹ was then inserted into the *SmaI* site of the *mmpL7* fragment. The 3.6-kb *NorI/SpeI* fragment containing *mmpL7::hyg* was excised from pcDNA2.1 and inserted into the same sites of pPR23-1 (ref. 28). Transformation and selection procedures were as described previously²⁸. To generate *attB::pks1-15*, we initially sub-cloned a 6.5-kb *XbaI/XmnI* fragment containing *pks1-15* from the appropriate H37RV BAC clone (provided by R. Brosch) into *EcoRV/XbaI*-restricted pBluescript II SK (Stratagene). The resultant plasmid was digested with *NorI/BamHI* into which the HN878 *pks15* sequence (including the *pks1-15* junction) generated by polymerase chain reaction (PCR) was inserted. The entire *pks1-15* insert was excised with *DraI/HindIII*, cloned into pMV361 (ref. 25) and transformed into HN878 *pks1-15::hyg*.

Biochemical analysis

Cultures were grown to an absorbance of 0.25 at 650 nm (*A*₆₅₀) at which point 0.1 μCi ml⁻¹ [1-¹⁴C]propionic acid or 0.7 μCi ml⁻¹ [ring-¹⁴C(U)]4-hydroxybenzoic acid (American Radiolabelled Chemicals) were added and incubated for a further 48 and 96 h, respectively. Cell pellets were re-suspended in MeOH:0.3% NaCl (aq.) (10:1) and apolar lipids extracted twice with petroleum ether as described³⁰. Filtered (0.2 μM) culture supernatants were extracted twice with 0.5 volumes of petroleum ether. Lipid extracts were analysed on Silica Gel-60 TLC plates (Merck) and developed in CHCl₃:MeOH (94:6). For two-dimensional TLC, plates were developed in CHCl₃:MeOH (95:5) (1st dimension) and toluene:acetone (70:30) (2nd dimension). TLC plates were visualized using a Storm 860 PhosphorImager (Molecular Dynamics). For *in vitro* studies, approximately 1 mg of PGL was extracted and purified from 2-1 cultures of HN878 by preparative Silica Gel TLC. One-dimensional ¹H-NMR spectroscopy was carried out on the purified material using a Mercury 300 MHz instrument and VNMR 6.1c software (Varian) with CDCl₃ as solvent and tetramethylsilane as an internal reference.

Animal studies

Before infection, *M. tuberculosis* cultures were adjusted to *A*₆₅₀ of 0.5 and stored at -70 °C as 20% glycerol stocks. Inocula were prepared by diluting these stocks to 4 × 10⁶ c.f.u. ml⁻¹ in PBS/Tween-80 (0.05%). Six-week-old B6D2 F₁ (C57BL/6 × DBA/2; F₁ progeny) mice (Taconic) were infected (30 mice per group) via aerosol for 10 min using a BioAerosol Nebulizing Generator (CH Technologies). In this manner, approximately 50–100 c.f.u. per lung were implanted as confirmed by homogenizing lungs (4 mice per group) in 7H9/ADC at 3 h after infection and plating for c.f.u. determination. Additional mice were killed at 2, 5 and 12 weeks after infection and serial dilutions of lung and spleen homogenates were plated. The log-rank test was used to determine statistical significance of survival differences observed in mice (GraphPad Prism v3.0).

Cytokine analysis

To generate BMMs, bone marrow flushed from mouse femurs (B6D2 F₁) was cultured for 7 days in high glucose DMEM (Gibco) supplemented with 20% FCS, 1 mM pyruvate, 2 mM glutamine and 30% L929 conditioned medium. 10⁶ BMMs (in high glucose DMEM plus 10% FCS, 1 mM pyruvate and 2 mM glutamine) seeded into 24-well plates were infected with various *M. tuberculosis* strains at a ratio of 1:1 for 4 h after which extracellular bacteria were removed by repeated washing with PBS. Culture supernatants were removed 18–24 h after infection, centrifuged and analysed for the presence of TNF-α, IL-6, IL-12 and MCP-1 by enzyme-linked immunosorbent assay (ELISA) (R&D Systems). Infected cells were lysed with 0.025% SDS and serial dilutions plated for c.f.u. determinations. Purified PGL (1 μg or 10 μg) and crude apolar lipid extracts (5 μg) prepared from HN878 *pks1-15::hyg* or H37Rv were re-suspended in petroleum ether, added to 24-well tissue culture plates and the solvent allowed to evaporate before adding BMMs as above. Additionally, similar assays were carried out in the presence of purified PDIM or *M. bovis* (BCG) PGL. Each infection or lipid treatment was performed in triplicate with macrophages prepared from at least three individual mice.

Received 7 May; accepted 13 July 2004; doi:10.1038/nature02837.

1. Tiruvilumala, P. & Reichman, L. B. Tuberculosis. *Annu. Rev. Publ. Health* **23**, 403–426 (2002).
2. Sreevatsan, S. *et al.* Restricted structural gene polymorphism in the *Mycobacterium tuberculosis* complex indicates evolutionarily recent global dissemination. *Proc. Natl Acad. Sci. USA* **94**, 9869–9874 (1997).
3. Fleischmann, R. D. *et al.* Whole-genome comparison of *Mycobacterium tuberculosis* clinical and laboratory strains. *J. Bacteriol.* **184**, 5479–5490 (2002).
4. North, R. J., Ryan, L., LaCourse, R., Mogues, T. & Goodrich, M. E. Growth rate of mycobacteria in mice as an unreliable indicator of mycobacterial virulence. *Infect. Immun.* **67**, 5483–5485 (1999).
5. Manca, C. *et al.* *Mycobacterium tuberculosis* CDC1551 induces a more vigorous host response *in vivo* and *in vitro*, but is not more virulent than other clinical isolates. *J. Immunol.* **162**, 6740–6746 (1999).
6. Manca, C. *et al.* Virulence of a *Mycobacterium tuberculosis* clinical isolate in mice is determined by failure to induce Th1 type immunity and is associated with induction of IFN-α/β. *Proc. Natl Acad. Sci. USA* **98**, 5752–5757 (2001).
7. Valway, S. E. *et al.* An outbreak involving extensive transmission of a virulent strain of *Mycobacterium tuberculosis*. *N. Engl. J. Med.* **338**, 633–639 (1998).
8. Bifani, P. J., Mathema, B., Kurepina, N. E. & Kreiswirth, B. N. Global dissemination of the *Mycobacterium tuberculosis* W-Beijing family strains. *Trends Microbiol.* **10**, 45–52 (2002).
9. Glynn, J. R., Whiteley, J., Bifani, P. J., Kremer, K. & van Soolingen, D. Worldwide occurrence of Beijing/W strains of *Mycobacterium tuberculosis*: a systematic review. *Emerg. Infect. Dis.* **8**, 843–849 (2002).

10. Cole, S. T. *et al.* Deciphering the biology of *Mycobacterium tuberculosis* from the complete genome sequence. *Nature* **393**, 537–544 (1998).
11. Manca, C. *et al.* Differential monocyte activation underlies strain specific *M. tuberculosis* pathogenesis. *Infect. Immun.* (in the press).
12. Cox, J. S., Chen, B., McNeil, M. & Jacobs, W. R. Jr Complex lipid determines tissue-specific replication of *Mycobacterium tuberculosis* in mice. *Nature* **402**, 79–83 (1999).
13. Sirakova, T. D., Thirumala, A. K., Dubey, V. S., Sprecher, H. & Kolattukudy, P. E. The *Mycobacterium tuberculosis* *pks2* gene encodes the synthase for the hepta- and octamethyl-branched fatty acids required for sulfolipid synthesis. *J. Biol. Chem.* **276**, 16833–16839 (2001).
14. Constant, P. *et al.* Role of the *pks15/1* gene in the biosynthesis of phenolglycolipids in the *Mycobacterium tuberculosis* complex. Evidence that all strains synthesize glycosylated p-hydroxybenzoic methyl esters and that strains devoid of phenolglycolipids harbor a frameshift mutation in the *pks15/1* gene. *J. Biol. Chem.* **277**, 38148–38158 (2002).
15. Marmiesse, M. *et al.* Macro-array and bioinformatic analyses reveal mycobacterial 'core' genes, variation in the ESAT-6 gene family and new phylogenetic markers for the *Mycobacterium tuberculosis* complex. *Microbiol.* **150**, 483–496 (2004).
16. Kolattukudy, P. E., Fernandes, N. D., Azad, A. K., Fitzmaurice, A. M. & Sirakova, T. D. Biochemistry and molecular genetics of cell-wall lipid biosynthesis in mycobacteria. *Mol. Microbiol.* **24**, 263–270 (1997).
17. Vergne, I. I. & Daffe, M. Interaction of mycobacterial glycolipids with host cells. *Front. Biosci.* **3**, 865–876 (1998).
18. Hunter, S. W. & Brennan, P. J. A novel phenolic glycolipid from *Mycobacterium leprae* possibly involved in immunogenicity and pathogenicity. *J. Bacteriol.* **147**, 728–735 (1981).
19. Mehra, V., Brennan, P. J., Rada, E., Convit, J. & Bloom, B. R. Lymphocyte suppression in leprosy induced by unique *M. leprae* glycolipid. *Nature* **308**, 194–196 (1984).
20. Fournie, J.-J., Adams, E., Mullins, R. J. & Basten, A. Inhibition of human lymphoproliferative responses by mycobacterial phenolic glycolipids. *Infect. Immun.* **57**, 3653–3659 (1989).
21. Vachula, K., Holzer, T. J. & Andersen, B. R. suppression of monocyte oxidative responses by phenolic glycolipid 1 of *Mycobacterium leprae*. *J. Immunol.* **142**, 1696–1701 (1989).
22. Silva, C. L., Faccioli, L. H. & Foss, N. T. Suppression of human monocyte cytokine release by phenolic glycolipid-1 of *Mycobacterium leprae*. *Int. J. Lepr.* **61**, 107–108 (1993).
23. Hashimoto, K. *et al.* *Mycobacterium leprae* infection in monocyte-derived dendritic cells and its influence on antigen-presenting function. *Infect. Immun.* **70**, 5167–5176 (2002).
24. Ng, V. *et al.* Role of the cell wall phenolic glycolipid-1 in the peripheral nerve predilection of *Mycobacterium leprae*. *Cell* **103**, 511–524 (2000).
25. Stover, C. K. *et al.* New use of BCG for recombinant vaccines. *Nature* **351**, 456–460 (1991).
26. Gordon, S. Alternative activation of macrophages. *Nature Rev. Immunol.* **3**, 23–35 (2003).
27. Garbe, T. R. *et al.* Transformation of mycobacterial species using hygromycin resistance as selectable marker. *Microbiol.* **140**, 133–138 (1994).
28. Pelicic, V. *et al.* Efficient allelic exchange and transposon mutagenesis in *Mycobacterium tuberculosis*. *Proc. Natl Acad. Sci. USA* **94**, 10955–10960 (1997).
29. O'Gaora, P. *et al.* Mycobacteria as immunogens: development of expression vectors for use in multiple mycobacterial species. *Med. Princ. Prac.* **6**, 91–96 (1997).
30. Slayden, R. A. & Barry, C. E. III in *Mycobacterium tuberculosis protocols* (eds Parish, T. & Stoker, N. G.) 229–245 (Humana, New Jersey, 2001).

Acknowledgements The authors wish to thank J. Gonzales and M. Goodwin for their assistance with animal studies and NMR spectroscopy, respectively. G.K. is supported by grants from the NIH.

Competing interests statement The authors declare that they have no competing financial interests.

Correspondence and requests for materials should be addressed to C.E.B. (clifton_barry@nih.gov).

Involvement of targeted proteolysis in plant genetic transformation by *Agrobacterium*

Tzvi Tzfira, Manjusha Vaidya & Vitaly Citovsky

Department of Biochemistry and Cell Biology, State University of New York, Stony Brook, New York 11794-5215, USA

Genetic transformation of plant cells by *Agrobacterium* represents a unique case of trans-kingdom DNA transfer¹. During this process, *Agrobacterium* exports its transferred (T) DNA and several virulence (Vir) proteins into the host cell², within which T-DNA nuclear import is mediated by VirD2 (ref. 3) and VirE2 (ref. 4) and their host cell interactors ATKAP-α⁵ and VIP1 (ref. 6), whereas its integration is mediated mainly by host cell proteins^{7–9}.